Bench-NPIN: Benchmarking Non-prehensile Interactive Navigation

Ninghan Zhong, Steven Caro*, Avraiem Iskandar*, Megnath Ramesh*, and Stephen L. Smith

***Abstract*— Mobile robots are increasingly deployed in unstructured environments where obstacles and objects are movable. Navigation in such environments is known as interactive navigation, where task completion requires not only avoiding obstacles but also strategic interactions with movable objects. Non-prehensile interactive navigation focuses on non-grasping interaction strategies, such as pushing, rather than relying on prehensile manipulation. Despite a growing body of research in this field, most solutions are evaluated using case-specific setups, limiting reproducibility and cross-comparison. In this paper, we present Bench-NPIN, the first comprehensive benchmark for non-prehensile interactive navigation. Bench-NPIN includes multiple components: 1) a comprehensive range of simulated environments for non-prehensile interactive navigation tasks, including navigating a maze with movable obstacles, autonomous ship navigation in icy waters, box delivery, and area clearing, each with varying levels of complexity; 2) a set of evaluation metrics that capture unique aspects of interactive navigation, such as efficiency, interaction effort, and partial task completion; and 3) demonstrations using Bench-NPIN to evaluate example implementations of established baselines across environments. Bench-NPIN is an open-source Python library with a modular design. The code, documentation, and trained models can be found at https://github.com/IvanIZ/BenchNPIN.**

I. Introduction

When mobile robots are deployed in cluttered and unstructured environments, such as homes, hospitals, or disaster sites, the ability for robots to interact with objects and obstacles can be essential for task completion. Traditional approaches to robot navigation focus on computing collision-free paths. However, in environments where obstacles block all feasible routes, robots must interact with obstacles to progress, leading to a class of problems known as Navigation Among Movable Obstacles (NAMO) [1]. Interactive navigation expands upon NAMO by including scenarios where interactions with objects in the environment are not only inevitable but essential for task completion, for example, pushing objects to designated locations while avoiding unnecessary collisions.

Historically, interactive navigation and NAMO have been studied with the assumption that mobile robots are equipped with manipulators to move obstacles out of the way [2], [3], [4], [5]. However, manipulators are not always viable due to cost considerations, structural limitations, or task-specific constraints. Moreover, prehensile manipulation of objects with complex dynamics remains a significant challenge. This has spurred increasing interest in non-prehensile interactive navigation (NPIN), where robots interact with objects with non-grasping actions [6], [7], [8], [9]. Despite the growing body of work, the field still lacks a unified framework for systematic evaluation and reproducibility, as no standardized benchmarking tools exist.

To address this gap, we present Bench-NPIN, the first comprehensive suite of tools for standardized training and evaluation of algorithms for non-prehensile interactive navigation. Bench-NPIN is made available as an open-source Python library. In this benchmark, we define two classes of non-prehensile interactive navigation tasks. *Navigation-centric NPIN* refers to the tasks where the objective is to navigate the robot to a goal location; *Manipulation-centric NPIN* refers to the tasks where the primary objective is to manipulate movable objects using a non-prehensile manipulator (e.g., pushed using the robot's front bumper) to reach a desired goal configuration.

Our key contributions are as follows. First, we introduce Bench-NPIN, a benchmarking tool, that consists of a range of simulated environments for both navigation-centric and manipulation-centric NPIN tasks. Each environment is user-configurable to modify the difficulty of the environments and the tasks. The included environments are as follows:

- navigating a maze among movable obstacles,
- autonomous ship navigation in ice-covered waters,
- delivering boxes to a receptacle, and
- clearing boxes from an area.

Secondly, we propose a set of novel metrics that are included in Bench-NPIN to evaluate and compare policies that tackle navigation-centric and manipulation-centric NPIN tasks. The proposed metrics capture properties unique to interactive navigation such as efficiency and interaction trade-offs, and partial task completions.

Finally, we demonstrate Bench-NPIN using established baseline algorithms for each task and present their evaluation results. The baseline implementations are included in Bench-NPIN as reference implementations for users to configure algorithms of their choosing. For our baselines, we include implementations of widely used Reinforcement Learning (RL) algorithms, such as Soft Actor-Critic (SAC) [10] and Proximal Policy Optimization (PPO) [11]. In addition to general RL baselines, we also include task-specific state-of-the-art methods, such as ship path planners [12], [13] for autonomous ship navigation and Spatial Action Maps [8] for manipulation-centric tasks.

*denotes equal contribution as the second authors.

This work is supported in part by the National Research Council Canada (NRC) and in part by the Natural Sciences and Engineering Research Council of Canada (NSERC).

Resources used in preparing this research were provided, in part, by the Province of Ontario, the Government of Canada through CIFAR, and companies sponsoring the Vector Institute.

The authors are with Department of Electrical and Computer Engineering, University of Waterloo, Waterloo, ON N2L 3G1, Canada (e-mails: {n5zhong, steven.caro, avraiem.iskandar, m5ramesh, stephen.smith}@uwaterloo.ca)

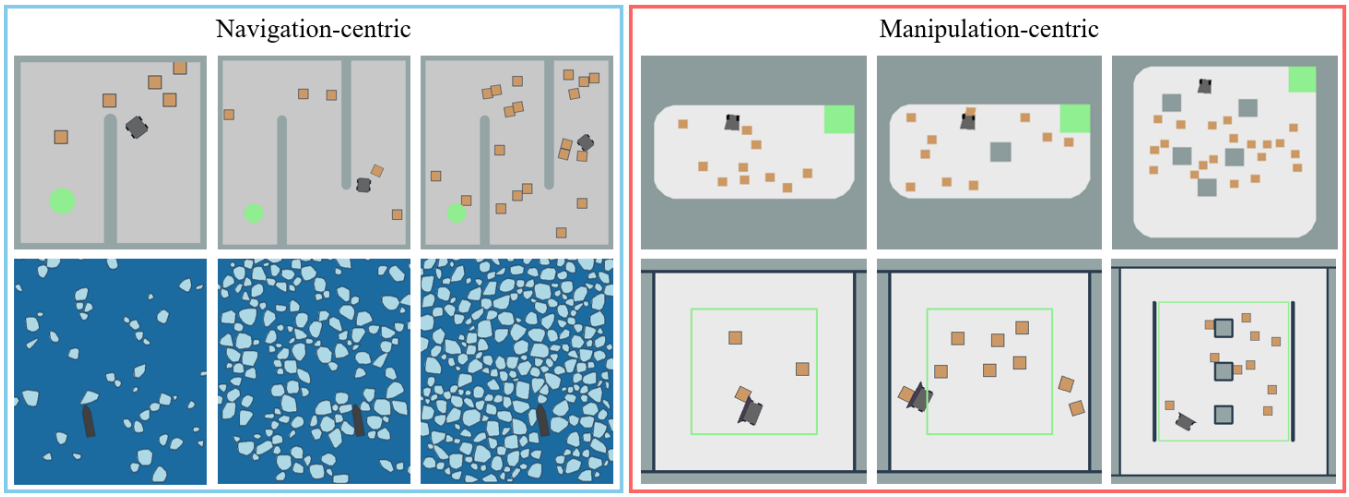

Fig. 1: Illustration of non-prehensile interactive navigation environments with configurable complexity levels. Upper-left shows the *Maze* environment, the mobile robot must reach the goal point among movable obstacles. Lower-left shows the *Ship-Ice* environment where an autonomous ship must navigate through ice-covered waters. Upper-right shows *Box-Delivery* environment, where the robot's objective is to push all boxes into the green receptacle. Lower-right is the *Area-Clearing* environment, where a robot needs to remove all boxes from within a clearance area outlined by the green rectangle.

II. Related Work

In this section, we review related work in NPIN and the most closely related benchmarks.

A. Non-prehensile Interactive Navigation

Interactive navigation [14] refers to scenarios where a mobile robot must interact with the environment to complete its tasks. Non-prehensile interactive navigation (NPIN) is a subset of this problem, where robots interact with obstacles and objects without using manipulators or grasping actions. NPIN tasks can be further classified into two categories: navigation-centric NPIN and manipulation-centric NPIN.

Navigation-centric NPIN focuses on reaching a goal location while engaging in inevitable environment interactions, such as pushing path-blocking obstacles aside. Prior work has explored various strategies to tackle this challenge. For instance, [7] investigated reinforcement learning-based navigation in cluttered environments with movable obstacles, proposing a local path-planning framework for dynamic interactions. [6] introduced an adaptive dynamics model for common indoor movable objects that enables robots to anticipate and adjust to object movements. Beyond terrestrial robots, [12], [13] studied autonomous surface vehicle (ASV) navigation in ice-covered waters, where ship-ice interactions are inevitable, and proposed planning frameworks that reduce collisions during navigation.

Manipulation-centric NPIN, on the other hand, emphasizes manipulating the movable objects in the environment to reach a desired configuration. Examples include pushing objects to predefined locations or clearing debris from a designated area. In [8], Spatial Action Map (SAM) is proposed as a novel action representation for a multi-object pushing problem, where a mobile robot must transport scattered objects into a goal receptacle. This work was subsequently extended in [15], where the robot uses an onboard pneumatic blower to clear up scattered objects. In [9], a Deep Reinforcement Learning (DRL) framework with task-space decomposition is proposed to address long-distance non-prehensile object delivery. In [16], curriculum reinforcement learning is deployed to learn multi-robot non-prehensile heavy object transportation.

B. Benchmarks for Robot Navigation

Various benchmarks have been proposed for mobile robot navigation. Traditional benchmarks focus primarily on collision-free navigation. [17] proposed a benchmark for ground mobile robot navigation in cluttered environments. [18] and [19] extend beyond static environments by considering both static and dynamic obstacles. [20] introduced SOCIALGYM for robots navigating dynamic human environments. However, these benchmarks primarily assess navigation performance under constraints that discourage environmental interaction, classifying collisions as failures rather than controlled contacts.

The Interactive Gibson Benchmark [14] represents an advancement in benchmarking interactive navigation, introducing scenarios where environmental interaction is necessary. Our work differs from [14] by focusing on non-prehensile interaction navigation. Further, we extend beyond navigation-centric scenarios considered in [14] by covering a broader range of tasks, including manipulation-centric scenarios such as non-prehensile object delivery via pushing.

Evaluation metrics in existing navigation benchmarks [17], [18] primarily focus on navigation success rates, collision count, and path efficiency. However, these metrics are insufficient for assessing interactive navigation tasks, where controlled interactions are required rather than avoided. [14] proposed a novel set of metrics for interactive navigation that captures both efficiency and environment disturbance from the interaction. These metrics are geared toward navigation-centric NPIN, and are not suitable for manipulation-centric cases where modifying the environment is part of the

task (i.e., box delivery). In contrast, our benchmark introduces separate evaluation metrics for navigation-centric and manipulation-centric NPIN, ensuring that interaction quality and efficiency are appropriately measured in both classes.

III. Bench-NPIN

Bench-NPIN consists of three main components – (i) environment, (ii) policy, and (iii) evaluation metrics. In this section, we detail the specifics of these environments, explain the implementation of custom policies in Bench-NPIN and introduce the metrics used to evaluate policies. First, we clarify some of the terminology used in this section.

Environment: An environment is a custom-built Gymnasium [21] interface. Each environment has multiple variations with increasing complexity (see Fig. 1). Environments can be run independent of a training session, and the robot can be manually operated by a user.

Task: We refer to a task as the robot's objective in a given environment. Specifically, we consider two types of tasks:

- *Navigation-centric*, where the robot must reach a specified goal region in the environment.
- *Manipulation-centric*, where the robot must move objects in the environment to specified areas.

Policy: A policy is a set of rules used to control the robot in an environment. It takes a sequence of observations as an input and outputs a robot action. In Bench-NPIN, we include several baseline policies as reference implementations to users, which are listed in Table I.

Metric: A metric is a score used to evaluate the effectiveness of a policy in completing a task in a given environment. In Section III-C, we introduce novel metrics that we included in Bench-NPIN to evaluate and compare policies.

A. Bench-NPIN Environments

We now introduce the navigation-centric and manipulation-centric environments and tasks included in Bench-NPIN. For each environment, we provide details about the actions and observations available to the robot and the rewards the robot receives. Table II summarizes the action space, observation space, and reward functions for each environment. Additional running illustrations of the environments can be found in the supplemental video.

1) Navigating maze with movable obstacles (Maze): The *Maze* environment features a static maze structure with randomly initialized obstacles. The robot's task is to navigate from a starting position to a goal location (green circle in Fig. 2) while minimizing path length and obstacle collisions. Variations of the environment include different maze structures, obstacle geometries, and obstacle locations and densities.

The robot in this environment is configured to move with a constant forward speed and receives an angular velocity as action input from the policy. At each timestep, the robot makes a local egocentric observation consisting of four channels that correspond to (i) static obstacle occupancy, (ii) movable obstacle occupancy, (iii) robot footprint, and (iv) a distance transform (DT) originating from the goal (goal DT). Fig. 2 shows an example of the robot's observations. The robot receives rewards for moving closer to the goal, penalties for colliding with obstacles, and a terminal reward when reaching the goal.

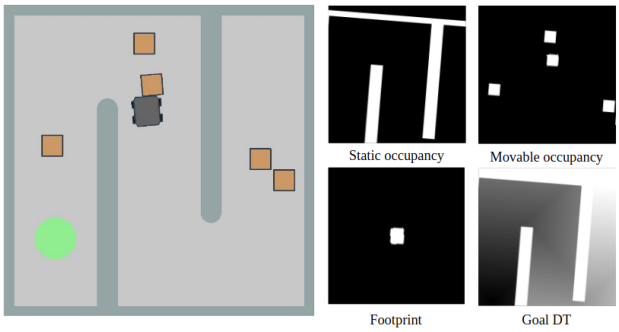

Fig. 2: The *Maze* environment (left) and an example egocentric observation for *Maze* (right).

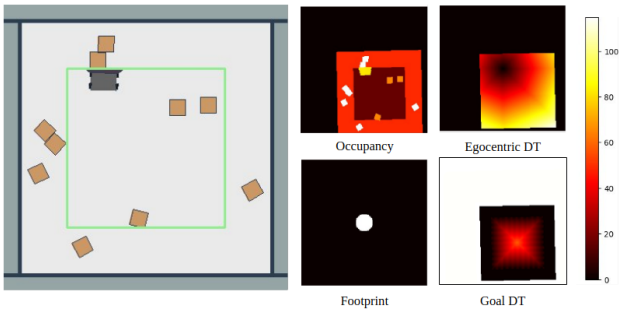

Fig. 3: The *Area-Clearing* environment (left) and example observation for *Area-Clearing* (right).

2) Autonomous ship navigation in icy waters (Ship-Ice): The *Ship-Ice* environment simulates an autonomous ship navigating in a channel of ice-covered waters (see Fig. 1). The ship's task is to reach a horizontal goal line ahead of the ship while minimizing collisions with broken ice floes in the channel [12]. The ice floes are represented as convex polygons with ice concentrations varying between 0% and 50%. As concentrations exceed approximately 20%, collision-free paths become non-existent, so the ship must minimize kinetic energy loss and maintain momentum.

Similar to the *Maze* environment, the ship moves with a constant forward speed and receives an angular velocity as action input. The ship makes the observations similar to *Maze* but with an additional channel that encodes the heading of the ship as a single-pixel-width line. This channel facilitates fine-grained movement around clusters of ice floes. The ship's reward function combines penalties for collisions with ice floes, a heading reward to encourage approaching the goal line, and a terminal reward for reaching the goal.

3) Delivering boxes to a receptacle (Box-Delivery): The *Box-Delivery* environment consists of a set of movable boxes and a designated *receptacle*. The robot is tasked with delivering all boxes to the receptacle using a non-prehensile manipulator (e.g. front bumper) to push the boxes. The boxes and robot starting location are randomly generated within an environment. Further variations are possible by including static obstacles (e.g., columns) and changing the number and size of movable objects.

TABLE I: Non-prehensile interactive navigation tasks in Bench-NPIN.

Environments	Task Class	Variations	Baselines Evaluated
Maze	Navigation-centric	maze complexity, obstacle count	SAC [10], PPO [11]
Ship-Ice	Navigation-centric	ice concentrations	SAC [10], PPO [11], ASV planning [12], [13]
Box-Delivery	Manipulation-centric	w/o static obstacles, box count	SAC [10], PPO [11], SAM [8]
Area-Clearing	Manipulation-centric	w/o static obstacles, box count	SAC [10], PPO [11], SAM [8], GTSP (Appendix I)

TABLE II: Rewards, actions and observations for each task.

Environments	Action	Observation	Rewards
Maze	Angular vel.	occupancy + footprint + goal DT	collision + distance decrement + terminal
Ship-Ice	Angular vel.	occupancy + footprint + goal DT + heading encoding	collision + heading + terminal
Box-Delivery	Heading	occupancy + footprint + egocentric DT + goal DT	collision + box completion + box displacement
Area-Clearing	Heading	occupancy + footprint + egocentric DT + goal DT	collision + box completion + box displacement

At each step, the robot receives a heading as its action input, in which case the robot travels for a fixed distance along that heading. The robot's observation is egocentric and includes (i) occupancy of the environment with static and movable objects encoded in different values, (ii) robot footprint, (iii) DT originating from the robot (egocentric DT), and (iv) DT originating from the receptacle (goal DT). The robot receives rewards for moving boxes toward the receptacle or delivering a box, and penalties when colliding with static obstacles or moving boxes away from the receptacle.

4) Clearing boxes from an area (Area-Clearing): The *Area-Clearing* environment consists of a set of movable boxes and a *clearance area*. The task of the robot is to remove the boxes from within this clearance area, with no constraints on the final positions of the cleared boxes. Variations of this environment can be created in Bench-NPIN by changing the number of objects to be removed, the number of static obstacles, and workspace constraints (e.g., walls blocking clearance area close to the boundary).

The robot actions and observations in *Area-Clearing* are identical to those of *Box-Delivery*. Fig. 3 illustrates the environment and corresponding robot observations. The robot (grey) pushes movable objects (brown) out from within a clearance area (inside light green square). In the occupancy observation, cleared boxes are shown in a distinct color from those still inside the area, visually indicating task progress. The reward function is constructed similar to the *Box-Delivery*, where the robot receives a reward when moving any object inside the clearance area closer to the boundary, and when pushing a box out of the boundary.

B. Bench-NPIN Implementation

Bench-NPIN is designed with a modular architecture to support flexible customization and ease of use. The benchmark has been designed with a one-line install to allow researchers to get up-and-running quickly. We highlight two core aspects of Bench-NPIN's implementation, which enable users to integrate custom policies of their choice to tackle the discussed NPIN tasks.

1) Gymnasium Integration: All environments detailed in Sec. III-A are implemented on top of the Pymunk 2D [22] physics engine. We integrate these environments within the Gymnasium [21] interface to standardize policy development and evaluation. The implementation supports a wide range of environment parameters through either script-level configuration or command-line arguments.

2) Extensible Policy Class: Bench-NPIN provides a standardized, extensible policy template to simplify the incorporation of new algorithms. This template follows a plug-and-play philosophy: a user only needs to implement the required APIs within a policy class. Bench-NPIN then handles inference, evaluation, and logging processes.

By way of illustration, Bench-NPIN comes with reference implementations for well-established baselines, as described in Sec. IV. These examples demonstrate both how to integrate popular Reinforcement Learning algorithms from Stable Baselines 3 [23] and how to incorporate specialized or state-of-the-art approaches. Additional documentation and usage examples, including configuration files and training scripts, are provided in the project repository at https://github.com/IvanIZ/BenchNPIN.

C. Metrics

We now provide a set of novel metrics to evaluate policies for NPIN tasks. These metrics are inspired by [14] and aim to capture the efficiency and interaction efforts of the robot. Let K be the number of movable objects in the environment. The mass and motion distance for each object are denoted as m_i and l_i for $i \in \{1, \dots, K\}$, respectively. We denote the mass and motion distance of the robot as m_0 and l_0, respectively. Since navigation-centric and manipulation-centric NPIN tasks are intrinsically different, Bench-NPIN provides two sets of metrics to address each class separately.

1) Navigation-centric Metrics: Efficiency in navigation-centric NPIN is computed with respect to the length of the robot's path. Let $\mathbb{1}_{\text{success}}$ be an indicator function on whether the robot successfully reaches the goal, and l_0^* be the shortest path distance from the robot's start position to the goal while ignoring interactions with movable objects. The efficiency score $E_{\text{nav}} \in [0, 1]$ is then computed as

$$E_{\text{nav}} = \mathbb{1}_{\text{success}} \frac{l_0^*}{l_0}. \tag{1}$$

Eq. 1 implies that the efficiency score $E_{\text{nav}} = 1$ if the robot reaches the goal with the shortest travel distance.

The interaction effort score measures the kinematic effort exerted by the robot to move objects along the path that it had traversed. This score is given by the ratio between the

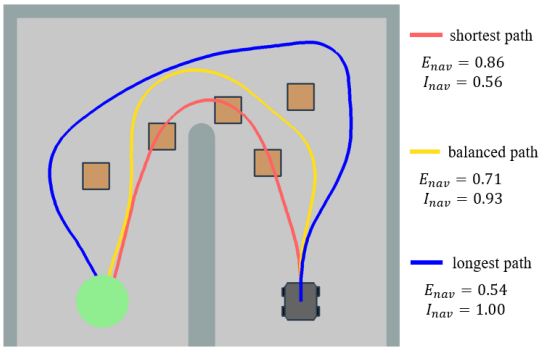

Fig. 4: An illustration of three teleoperated paths and the corresponding performance. While the shortest path (red) has the highest efficiency score $E_{\text{nav}} = 0.86$, the excessive collisions with the movable obstacles significantly degrade the effort score $I_{\text{nav}} = 0.56$. In contrast, while the longest path (blue) is collision-free $I_{\text{nav}} = 1.00$, efficiency is largely compromised $E_{\text{nav}} = 0.54$. A balanced path (yellow) potentially offers the best trade-off.

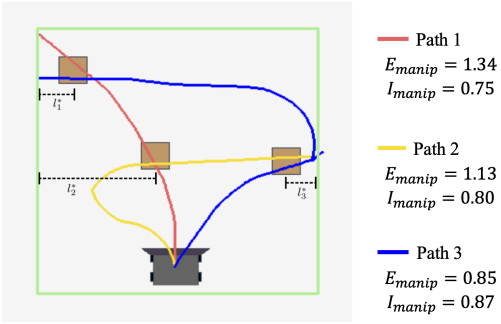

Fig. 5: Three teleoperated paths for area clearing, with each path having a task success score $S_{\text{manip}} = 2/3$. While path 1 (red) has the highest efficiency score, its effort score is low as it moves a box longer than its shortest distance to the goal (dotted lines of length l_i^*). In contrast, path 3 (blue) achieves the best effort score by pushing as little as possible, but results in a long path and a low efficiency score. Path 2 (yellow) potentially offers the best trade-off.

approximated minimum work and the approximated actual work done by the robot from overcoming kinetic frictional forces due to interactions in its path. To approximate this work, we assume that the entire environment has a kinetic friction coefficient μ. Following this, the kinetic frictional force for moving the ith object is $\mu m_i g$ and the work done by the robot to overcome this force (i.e., move this object) is $\mu m_i g l_i$. We further approximate the minimal work required by considering the robot as the 0th object, giving $\mu m_0 g l_0$. Thus, the interaction effort score $I_{\text{nav}} \in [0, 1]$ is computed as

$$I_{\text{nav}} = \frac{\mu m_0 g l_0}{\sum_{i=0}^{K} \mu m_i g l_i} = \frac{m_0 l_0}{\sum_{i=0}^{K} m_i l_i}. \tag{2}$$

Eq. 2 implies that the maximum interaction effort score is reached when the robot manages to reach the goal without moving any objects. Further, I_{nav} reduces when interacting with heavier objects at greater distances, an undesirable behavior in navigation-centric tasks. Fig. 4 illustrates how our metrics capture both efficiency and interaction effort. This visualization also highlights the inherent and unique trade-off in interactive navigation, where policies need to consider balancing both minimizing travel distance and avoiding unnecessary interactions.

2) Manipulation-centric Metrics: The metrics for manipulation-centric NPIN, unlike the navigation-centric NPIN metrics, must incorporate the minimum path length and effort required by the robot to manipulate objects towards completing its task. We also look to compare robot paths that may achieve *partial completion* of tasks, e.g., push two out of four boxes into the receptacle. To capture this effectively, we propose three metrics: (i) task success score S_{manip}, (ii) efficiency score E_{manip}, and (iii) interaction effort score I_{manip}.

To simplify our explanation, we consider that each of the K movable objects must be manipulated to a desired configuration (delivered or cleared). As such, the robot must complete a series of smaller manipulation *sub-tasks* corresponding to each box to complete the overall task. Let $\mathbb{1}^i_{\text{success}}$ be an indicator function that denotes whether the sub-task corresponding to the i^{th} movable object has been completed. Let $K' \leq K$ be the number of sub-tasks that have been completed successfully, i.e., $K' = \sum_{i=1}^{K} \mathbb{1}^i_{\text{success}}$. The task success score S_{manip} is given as

$$S_{\text{manip}} = \frac{K'}{K}. \tag{3}$$

Now, given that K' sub-tasks were completed, let $L^*(K')$ be the minimum path length required to complete the successful sub-tasks. For example, if the robot delivers 2 out of 4 boxes, $L^*(K')$ is the minimum path length the robot must take to move the two boxes to the receptacle. The efficiency score E_{manip} is given by

$$E_{\text{manip}} = \frac{L^*(K')}{l_0}. \tag{4}$$

In Bench-NPIN, we compute $L^*(K')$ using a minimum spanning tree (MST) of a graph G that we construct as follows. The vertex set includes K' vertices for the initial positions of the movable objects, another K' vertices for the closest point to the goal (receptacle or clearance area boundary) from each object, and a vertex for the robot. Edges are added between all pairs of objects, from the robot to each object, and from each object to its nearest goal, with the edge weights being the shortest distance between the two points. The MST of this graph is not a strict lower bound on the total path length, and as such, it is not guaranteed that $E_{\text{manip}} \in [0, 1]$. However, we find that this is a practical bound, as doubling the edges of the MST provides a path that can complete the sub-tasks (ignoring object-to-object interactions). Using both S_{manip} and E_{manip}, we can determine how many sub-tasks the robot has completed, and how efficient its path was to complete the sub-tasks.

For the interaction effort score, we look to approximate the minimum work the robot must do to complete K' sub-tasks while traversing its path. Using the friction coefficient μ of the environment, this work is approximated as $\mu g(m_0 l_0 + \sum_{i=1}^{K} \mathbb{1}^i_{\text{success}} m_i l_i^*)$, where l_i^* is the shortest distance from the i^{th} object to the goal (see Fig. 5). The actual work done by the robot is approximated as $\sum_{i=0}^{K} \mu m_i g l_i$, i.e., similar to the one in I_{nav}. Using this, the interaction effort score $I_{\text{manip}} \in [0, 1]$ is computed as

$$I_{\text{manip}} = \frac{m_0 l_0 + \sum_{i=1}^{K} \mathbb{1}^i_{\text{success}} m_i l_i^*}{\sum_{i=0}^{K} m_i l_i}. \tag{5}$$

Fig. 5 illustrates the manipulation-centric NPIN metrics capturing the efficiency and interaction effort for three trajectories for the area clearing task. All trajectories achieve a task success score of $2/3$, but with different trade-offs for path length and interaction effort.

IV. Evaluating Baselines using Bench-NPIN

In this section, we present experimental results for all interactive navigation tasks. These results are intended to confirm the extensibility of Bench-NPIN and provide benchmarking references for future studies.

A. Implemented Baselines

To support both general NPIN research and task-specific studies, Bench-NPIN includes a diverse set of baselines. These baselines fall into two categories: (i) reinforcement learning baselines applicable to all tasks outlined in Section III-A and (ii) task-specific baselines for each task. The baselines for each task are summarized in Table I. For each task, we test the corresponding baselines using a single configuration of the environment and evaluate their performance using the metrics from Section III-C.

The reinforcement learning baselines include Soft Actor-Critic (SAC) [10] and Proximal Policy Optimization (PPO) [11]. These baselines were implemented using Stable Baselines 3 [23] and trained across all tasks. To handle image observations, both baselines employ a customized ResNet18 [24] backbone with the last linear layer removed as the high-dimensional observation encoder, followed by a 3-layer MLP to output actions or value estimates.

In addition to general RL baselines, Bench-NPIN provides specialized policies tailored for individual tasks. For *Ship-Ice*, we provide lattice-planning [12] and predictive-planning [13] policies designed for ASV navigation. For *Box-Delivery* and *Area-Clearing*, we adopt the Spatial Action Map (SAM) policy [8], which is a method designed for multi-object pushing. The SAM policy learns to output a series of waypoints in the environment that enable the robot to complete a manipulation-centric task. To implement SAM, we also configured the *Box-Delivery* and *Area-Clearing* environments to receive waypoints in the environment as action inputs. Additionally, we introduce a Generalized Traveling Salesman Problem (GTSP) based policy (Appendix I) for *Area-Clearing* that plans a global path to clear all boxes given their initial states.

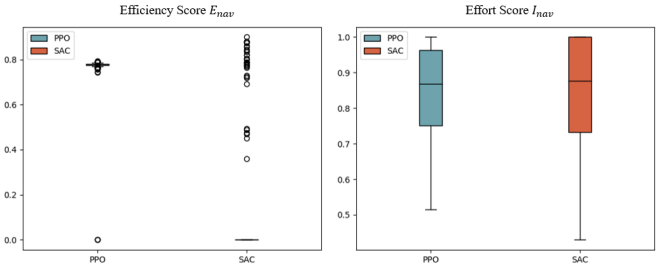

Fig. 6: Evaluation results for PPO and SAC in *Maze*.

Both SAC and PPO policies for all tasks are trained on a single 4GB NVIDIA GeForce RTX 3050 GPU for approximately 30 hours. For the manipulation-centric tasks, SAM was trained on NVIDIA RTX 6000 for approximately 7 hours. In each environment, we evaluated all baseline policies for 200 episodes. We fixed a constant random seed to evaluate each environment to ensure that all policies were tested against identical configurations.

B. Maze Evaluations

We evaluated the performance of SAC and PPO in a U-shaped maze with 5 movable obstacles, as shown in Fig. 4. The robot starts at the lower-right end of the maze and must reach the goal region located in the lower-left end. The obstacle placements are randomized at the start of each episode.

Fig. 6 shows the efficiency and interaction effort scores after evaluating PPO and SAC in *Maze*. Overall, PPO policy gives the best performance. The PPO policy achieves a mean efficiency of 0.76 and a mean effort score of 0.85. The SAC policy gives a comparable effort score (mean 0.84) to PPO (mean 0.85). However, it is important to note that SAC struggles to navigate the robot toward the goal in most episodes. This challenge is reflected in the efficiency score, where the majority of episodes display efficiency values concentrated near zero, as indicated by a narrow interquartile range and a median close to zero. This explains the high effort score for SAC, as the robot did not have many opportunities to interact with the movable objects, as was the case with PPO.

C. Ship-Ice Evaluations

In *Ship-Ice*, the performance of SAC, PPO, lattice-planning policy, and predictive-planning policy are evaluated in 10% ice concentration with a 10-meter goal horizon. In each episode, the ice floes are randomly generated up to 10% concentration, and the ship is randomly initialized along a start line 10 meters away from the goal line.

Fig. 7 shows the evaluation results for PPO, SAC, lattice-planning policy, and predictive-planning policy. All baselines perform comparably in terms of efficiency with scores close to $E_{\text{nav}} = 1.0$. This is potentially due to the fact that evaluations are performed under a low ice concentration, so scenarios where long detours are required for avoiding large clusters of ice take place less frequently. In terms of collision avoidance, SAC gives the highest interaction effort

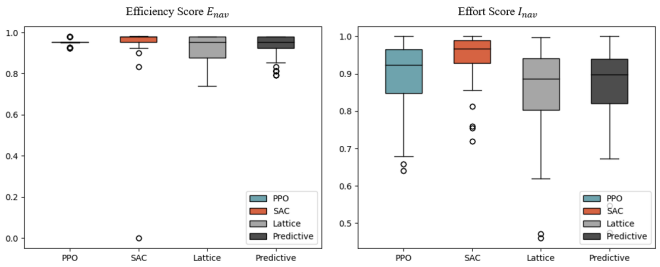

Fig. 7: Evaluation results for PPO, SAC, lattice-planning policy (Lattice), and predictive-planning policy (Predictive) in *Ship-Ice*.

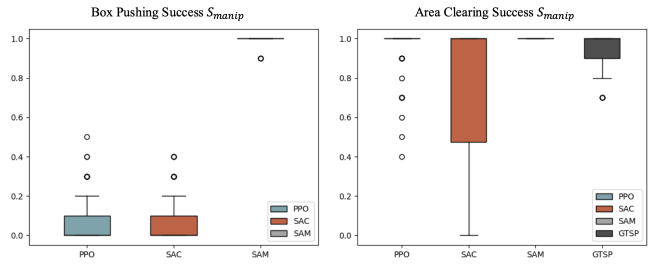

Fig. 8: Task success scores S_{manip} for the manipulation-centric NPIN baselines included in the benchmark.

scores, making it overall the best-performing model under 10% concentration setup.

D. Box-Delivery Evaluations

For *Box-Delivery*, we evaluated the performance of PPO, SAC, and SAM under the setting shown in the left-most *Box-Delivery* snapshot in Fig. 1, where the robot must deliver 10 boxes to the receptacle with no static obstacles impeding its path. The positions of the robot and boxes are randomly initialized at the start of an episode. The episode terminates after all boxes have been delivered, or if the robot does not deliver any boxes to the receptacle for 200 steps.

The results of evaluating the baseline policies are shown in Figs. 8 and 9. We observe that SAM drastically outperforms the other baselines in terms of success and efficiency. This is mainly because SAM is a specialized algorithm for manipulation-centric tasks, whereas PPO and SAC are general RL algorithms. Another difference is that the SAM policy learns to output waypoints for the robot to drive to, whereas PPO and SAC learn to output a heading. As such,

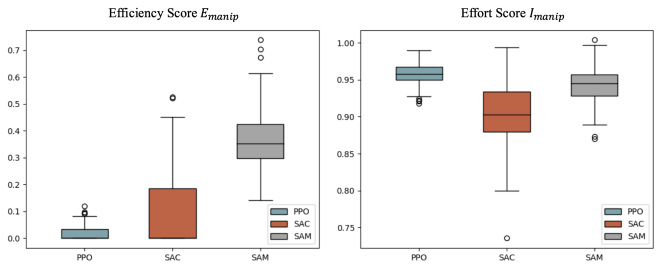

Fig. 9: Evaluation results for PPO, SAC, and SAM in *Box-Delivery*.

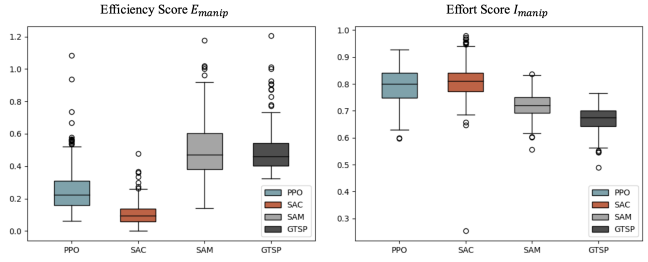

Fig. 10: Evaluation results for PPO, SAC, SAM, and GTSP in *Area-Clearing*.

SAM is able to learn a more effective policy than PPO and SAC within the provided training time as the mapping from the high-dimensional observation space to a series of waypoints is less complicated to learn than mapping to a series of headings.

E. Area-Clearing Evaluations

We now evaluate the performance of PPO, SAC, SAM, and GTSP (Appendix I) policies for the *Area-Clearing* environment. For this evaluation, we used the environment configuration where the robot must clear 10 boxes from within a rectangular clearance boundary without any static walls or obstacles blocking its path (Fig. 3). Each policy was run for 200 episodes, where the initial positions of the boxes are randomized after every episode. Also, the robot is initialized facing upwards at a random point close to the bottom of the environment. The episode terminates when all boxes are cleared out, or if the robot does not clear a box for 200 steps.

Figs. 8 and 10 show the results of evaluating the baseline policies from Table I. All baselines achieve high task success scores, with SAM outperforming all baselines as it successfully clears all boxes in every episode. We also observe that SAM outperforms all baselines in efficiency, while SAC achieves the best effort score. This is because the SAM policy prefers stacking multiple boxes and clearing them simultaneously, while the SAC policy results in long paths with relatively minimal interaction with the boxes. However, in comparison with the GTSP planner, SAM achieves better effort scores as it considers object-to-object interactions while stacking boxes and minimizes the distance traveled by the boxes (lower effort). In comparison, the GTSP policy does not consider this and results in accidental stacking of boxes, which increases the robot's effort (see Appendix I).

V. Conclusion and Future Work

This work introduces Bench-NPIN, the first comprehensive benchmark for non-prehensile interactive navigation. Bench-NPIN features various tasks in simulated environments divided into two categories: navigation-centric tasks and manipulation-centric tasks. Users can customize tasks with different levels of complexity. Additionally, the benchmark includes implementations of both established learning policies and task-specific policies for each task, demonstrating its extensibility. It also provides a set of metrics

specifically designed to measure efficiency and interaction effort within interactive navigation tasks.

Future work includes extending Bench-NPIN to allow collecting human demonstration data from the provided environments. This may enable the development of learning from demonstration (LfD) policies to tackle NPIN tasks. Bench-NPIN will also be extended to 3D environments with realistic sensor models and open-world dynamics. Finally, we plan to apply Bench-NPIN on real mobile robots to address sim-to-real gaps for interactive navigation research.

We acknowledge that it is challenging, or even impossible, to build a single benchmark that will suit the needs of all researchers in non-prehensile interactive navigation. However, we have been motivated by the importance of the area and the lack of existing benchmarks. There is significant potential for progress in NPIN, and learning-based algorithms show promise. As such, we hope that Bench-NPIN will provide a useful tool for researchers working in non-prehensile interactive navigation, and will facilitate further research and breakthroughs in the area.

APPENDIX I
GTSP BASELINE FOR AREA CLEARING

We provide details about the *Area-Clearing* baseline policy that computes a robot path by solving a generalized traveling salesman problem (GTSP). This GTSP policy is inspired by an approach for robot coverage path planning [25]. For each box in the environment, we consider the path to clear the box across each edge of the clearance area boundary. For example, in the case of a rectangular clearance boundary (Fig. 3), we consider 4 paths to clear each box across each of the 4 edges. We will refer to these as the box's *clearance paths*. We construct an auxiliary graph $G = (V, E)$ where each box constitutes a set S and contains vertices $v \in V$ that each correspond to a clearance path considered for the specific box. The robot's start position is encoded as a seperate vertex. The edge cost between two vertices is the shortest path length to reach the start of one clearance path from the end of another (or the robot's start position). Solving the GTSP on this graph gives us a robot path that aims to clear each box individually along a series of clearance paths. The path is computed once and executed by the robot until it either (i) clears all boxes in the environment or (ii) finishes the full path. Note that this method does not necessarily clear all boxes and does not minimize the robot's effort as it ignores object-to-object interactions.

REFERENCES

[1] K. Ellis, D. Hadjivelichkov, V. Modugno, D. Stoyanov, and D. Kanoulas, "Navigation among movable obstacles via multi-object pushing into storage zones," *IEEE Access*, vol. 11, pp. 3174–3183, 2023.

[2] M. Stilman and J. J. Kuffner, "Navigation among movable obstacles: Real-time reasoning in complex environments," *International Journal of Humanoid Robotics*, vol. 2, no. 04, pp. 479–503, 2005.

[3] A. Petrovskaya and A. Y. Ng, "Probabilistic mobile manipulation in dynamic environments, with application to opening doors." in *IJCAI*, 2007, pp. 2178–2184.

[4] M. Stilman, K. Nishiwaki, S. Kagami, and J. J. Kuffner, "Planning and executing navigation among movable obstacles," *Advanced Robotics*, vol. 21, no. 14, pp. 1617–1634, 2007.

[5] H.-C. Wang, S.-C. Huang, P.-J. Huang, K.-L. Wang, Y.-C. Teng, Y.-T. Ko, D. Jeon, and I.-C. Wu, "Curriculum reinforcement learning from avoiding collisions to navigating among movable obstacles in diverse environments," *IEEE Robotics and Automation Letters*, vol. 8, no. 5, pp. 2740–2747, 2023.

[6] C. Dai, X. Liu, K. Sreenath, Z. Li, and R. Hollis, "Interactive navigation with adaptive non-prehensile mobile manipulation," *arXiv preprint arXiv:2410.13418*, 2024.

[7] L. Yao, V. Modugno, A. M. Delfaki, Y. Liu, D. Stoyanov, and D. Kanoulas, "Local path planning among pushable objects based on reinforcement learning," in *2024 IEEE/RSJ International Conference on Intelligent Robots and Systems (IROS)*. IEEE, 2024, pp. 3062–3068.

[8] J. Wu, X. Sun, A. Zeng, S. Song, J. Lee, S. Rusinkiewicz, and T. Funkhouser, "Spatial action maps for mobile manipulation," *arXiv preprint arXiv:2004.09141*, 2020.

[9] G. Eoh, "Deep-reinforcement-learning-based object transportation using task space decomposition," *Sensors*, vol. 23, no. 10, p. 4807, 2023.

[10] T. Haarnoja, A. Zhou, P. Abbeel, and S. Levine, "Soft actor-critic: Off-policy maximum entropy deep reinforcement learning with a stochastic actor," in *International conference on machine learning*. PMLR, 2018, pp. 1861–1870.

[11] J. Schulman, F. Wolski, P. Dhariwal, A. Radford, and O. Klimov, "Proximal policy optimization algorithms," *arXiv preprint arXiv:1707.06347*, 2017.

[12] R. de Schaetzen, A. Botros, R. Gash, K. Murrant, and S. L. Smith, "Real-time navigation for autonomous surface vehicles in ice-covered waters," in *2023 IEEE International Conference on Robotics and Automation (ICRA)*. IEEE, 2023, pp. 1069–1075.

[13] N. Zhong, A. Potenza, and S. L. Smith, "Autonomous navigation in ice-covered waters with learned predictions on ship-ice interactions," *arXiv preprint arXiv:2409.11326*, 2024.

[14] F. Xia, W. B. Shen, C. Li, P. Kasimbeg, M. E. Tchapmi, A. Toshev, R. Martín-Martín, and S. Savarese, "Interactive gibson benchmark: A benchmark for interactive navigation in cluttered environments," *IEEE Robotics and Automation Letters*, vol. 5, no. 2, pp. 713–720, 2020.

[15] J. Wu, X. Sun, A. Zeng, S. Song, S. Rusinkiewicz, and T. Funkhouser, "Learning pneumatic non-prehensile manipulation with a mobile blower," *IEEE Robotics and Automation Letters*, vol. 7, no. 3, pp. 8471–8478, 2022.

[16] G. Eoh and T.-H. Park, "Cooperative object transportation using curriculum-based deep reinforcement learning," *Sensors*, vol. 21, no. 14, p. 4780, 2021.

[17] D. Perille, A. Truong, X. Xiao, and P. Stone, "Benchmarking metric ground navigation," in *2020 IEEE International Symposium on Safety, Security, and Rescue Robotics (SSRR)*. IEEE, 2020, pp. 116–121.

[18] Z. Xu, B. Liu, X. Xiao, A. Nair, and P. Stone, "Benchmarking reinforcement learning techniques for autonomous navigation," in *2023 IEEE International Conference on Robotics and Automation (ICRA)*. IEEE, 2023, pp. 9224–9230.

[19] L. Kästner, T. Bhuiyan, T. A. Le, E. Treis, J. Cox, B. Meinardus, J. Kmiecik, R. Carstens, D. Pichel, B. Fatloun *et al.*, "Arena-bench: A benchmarking suite for obstacle avoidance approaches in highly dynamic environments," *IEEE Robotics and Automation Letters*, vol. 7, no. 4, pp. 9477–9484, 2022.

[20] J. Holtz and J. Biswas, "Socialgym: A framework for benchmarking social robot navigation," in *2022 IEEE/RSJ International Conference on Intelligent Robots and Systems (IROS)*. IEEE, 2022, pp. 11 246–11 252.

[21] M. Towers, A. Kwiatkowski, J. Terry, J. U. Balis, G. De Cola, T. Deleu, M. Goulão, A. Kallinteris, M. Krimmel, A. KG *et al.*, "Gymnasium: A standard interface for reinforcement learning environments," *arXiv preprint arXiv:2407.17032*, 2024.

[22] V. Blomqvist, "Pymunk: A easy-to-use pythonic rigid body 2d physics library. (version 6.7.0)," 2024. [Online]. Available: https://pymunk.org

[23] A. Raffin, A. Hill, A. Gleave, A. Kanervisto, M. Ernestus, and N. Dormann, "Stable-baselines3: Reliable reinforcement learning implementations," *Journal of Machine Learning Research*, vol. 22, no. 268, pp. 1–8, 2021.

[24] K. He, X. Zhang, S. Ren, and J. Sun, "Deep residual learning for image recognition," in *Proceedings of the IEEE conference on computer vision and pattern recognition*, 2016, pp. 770–778.

[25] M. Ramesh, F. Imeson, B. Fidan, and S. L. Smith, "Anytime Replanning of Robot Coverage Paths for Partially Unknown Environments," *IEEE Transactions on Robotics*, vol. 40, pp. 4190–4206, 2024.